Wave runup estimates at gentle beaches in the northern Indian Ocean

Master's thesis in physical oceanography

Ahmed Alkarory Ahmed Abdalazeez

UNIVERSITY OF BERGEN

Faculty of Mathematics and Natural Sciences

Geophysical Institute

October 2012

To my parents

UNIVERSITY OF BERGEN

Abstract

Faculty of Mathematics and Natural Sciences

Geophysical Institute

Master of Science

by

Ahmed Alkarory Ahmed Abdalazeez

The aim of this study is to estimate the wave runup on selected beaches around the northern Indian Ocean. The runup has been estimated using ERA-Interim, which is the latest global atmospheric re-analysis produced by the European Centre for Medium-Range Weather Forecasts (ECMWF). ECMWF uses the global Wave Model (WAM) model to calculate two dimensional wave spectra.

The distances between the model grid points and the beaches have been calculated by a great circle calculator. The beach slopes have been calculated by Google Earth for all locations, except Maldives beach, which was assumed as an imaginary beach because the method of calculating the slope could not be used there. The significant wave height as well as the peak wave period at the grid points are assumed to be the same at the beach.

The most frequent estimated runup is between 0.5 m and 1.0 m, which is produced by swell coming from the southern Indian Ocean for all locations except Sri Lanka, India and Maldives shores, where the most frequent runup value is less than 0.5 m. However, the extreme wave runup occurs with the largest wave heights during summer monsoon in July. Generally, the high wave height depends on wind sea. The mean elevation of the runup for all locations is 0.56 m. It is comparable to the measured values obtained by (Stochdon et al., 2006) at several beaches in USA and the Netherlands who found the mean value of dissipative sites (84 cm) for all experiments.

Acknowledgements

First of all I thank God for making me meet and be around such great people who motivated me and this research project would not have been possible to be completed without their great support and courage. I would like to express the deepest appreciation to my supervisor, Dr. Knut Barthel, who has the attitude and the substance of a genius: He continually and convincingly conveyed a spirit of adventure in regard to research and scholarship, and an excitement in regard to teaching. Without his guidance and persistent help this dissertation would not have been possible. Deepest gratitude to, Dr. Øyvind Berivik at the Norwegian Weather service for getting the data and idea for this study, without whose knowledge and assistance this study would not have been successful.

I would like to thank my parents, brother and sisters, who gave me their unequivocal support throughout, as always, for which my mere expression of thanks likewise does not suffice.

A special thank of mine goes to my colleagues they helped me in completing the project. I would like to thank my Sudanese friends in Bergen, A special thank to my best friends Mohammed Salih, Mohammed Ali and Alfatih Ali for their support and encouragement.

I would also like to convey thanks to the Geophysical Institute – University of Bergen, and Institute of Marine Research at the Red Sea University for providing the financial means and library facilities. At last but not the least I want to thank my friends who appreciated me for my work and motivated me.

Contents

Chapter 1

Introduction

In modern years, the study of wave runup received considerable attention from researchers because of their direct effect on coastal structures and protection works (Nielsen and Hanslow, 1991). Wave runup is the extreme vertical height of the wave on a beach, and it is affected by the wave setup and swash (Vitousek et al., 2010).

Wave dynamics near the shore are very complex, and the ground water flow depends on the beach slope (Massel and Pelinovsky, 2001). When Ocean waves are approaching towards the beach, most of the wave energy is dissipated across the surf zone by waves breaking. A part of that energy is converted into potential energy as runup on the beach (Stochdon et al., 2006). The vertical displacement in wave runup consists of two components: Elevation of the mean water level above the still water level, which is called the wave setup (see Figure 1.1), and the fluctuations of that mean, which is called the swash (Ruggiero et al., 2004). In Figure 1.1a, the swash is given at times of extrema and the difference between the runup and the setup values. Based on statistics, extreme wave runup R_2 is the value of R that will exceed 2% of the time. The lowest vertical displacement below the still water level is called wave rundown (Gourlay, 1992).

Runup waves are important because their motion transmit much of the energy responsible for dune and beach erosion. Thus, studying the extreme runup is

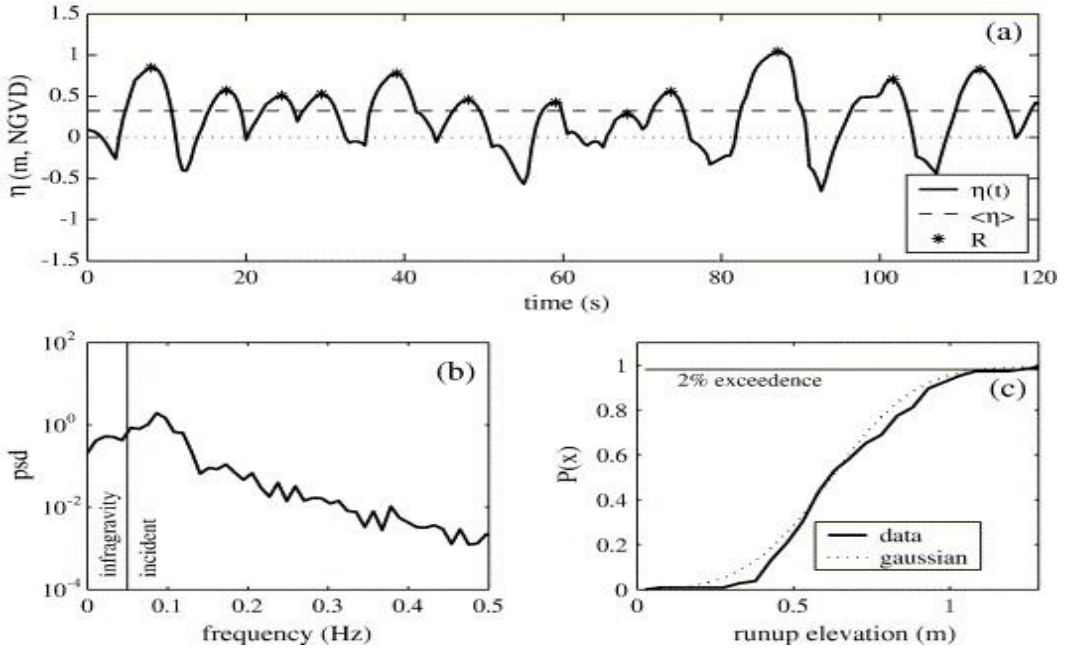

Figure 1.1: Water-level time series (a) indicating individual runup maxima, R, setup at the shoreline, ξ and swash excursion, S. Significant swash statistics, S, were calculated from the spectra (b) of the water-level time series. The 2% exceedance value of runup, R_2, was calculated from the cumulative PDF of the discrete measures of R (c). This figure is taken from Stochdon et al. (2006).

important for the accurate prediction of their effects on protective dunes and adjacent properties (Stochdon et al., 2006). Runup plays also an important role in the bioproductivity of sandy beaches and the functioning of a beach ecosystem. Thus, the runup process also helps to understand the relationship between natural variation and physical marine factors (Massel and Pelinovsky, 2001).

The available information concerning wave runup on coasts in the northern Indian Ocean is limited. It appears that, no single study has been reported on wave runup in this area. Thus, this study aims to estimate the wave runup on the natural beaches with gentle slopes around the northern Indian Ocean.

1.1 The area of study

The North Indian Ocean covers two interacting regions affected by wave climate:

1. The Equatorial region that extents to about 5°N – 8°N, which is dominant by wind local forcing

2. The Arabian Sea, which is dominant by strong southwesterly winds blowing during the summer monsoon (Kantha et al., 2008).

Swell coming from the southern Indian Ocean contributes significantly in determining the northern Indian Ocean wave climate. Besides the influence of the southwest summer monsoon winds, the swell dominates on the local wave climate in the Bay of Bengal but stronger in the Arabian Sea due to the strong southwest summer monsoon. During the rest of the year, the swell is a dominant part in determining the Indian Ocean wave climate (Sabique et al., 2012).

The map in Figure 1.2 shows the locations at which the runup wave study will be focused. At each location, a statistical analysis of extreme wave runup is made, which is based on 21 years of six-hourly wave height and wave period data.

The locations were selected to make small slopes in order to investigate the condition of the ratio (ξ), of beach slope to steepness wave which must be smaller than 0.3 to be considered as a dissipative wave runup. To calculate the appropriate distance on the beach and the elevation, Google earth was used to get the beach slope (β). Then $\tan\beta$ (see Table 2.1) was calculated. The beach slope for Maldives is considered as an imaginary beach since where we were not able to use this method to estimate its beach slope. According to Riyaz (2009), the Maldives islands are small and rarely reach more than 2.5 m above sea level, therefore, they are at risk of flooding, tsunami and sea level changes.

1.2 Indian monsoon

Heat variations cause oscillations in the northern and southern hemisphere pressure systems and drive changes in the seasonal winds (Woodberry et al., 1989). There are two seasonal winds affect the Indian Ocean: The southwest monsoon (summer monsoon) and the northeast monsoon (winter monsoon). Summer monsoon in the Indian Ocean is considered as one of the most dynamical interactions between atmosphere, ocean and continent (Sabique et al., 2012). The strong heating of the Asian continent compared to the Indian Ocean causes a strong surface

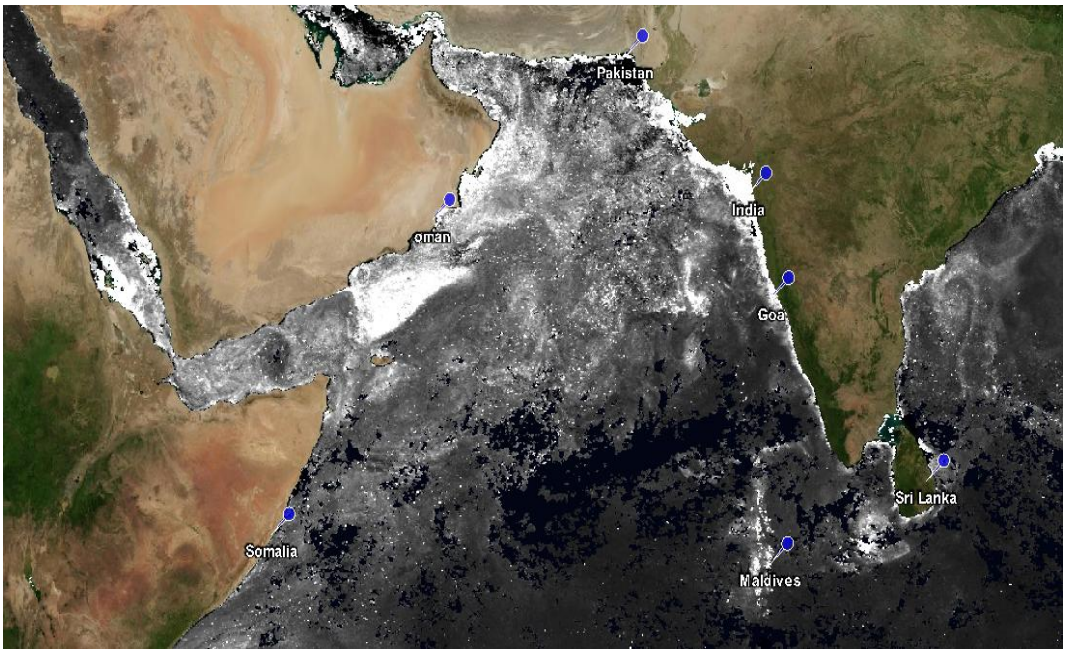

Figure 1.2: Location the beaches in this study.

pressure gradient which drives southwest winds during June, July and August, as shown in Figure 1.3 (Clemens and Prell, 1990). In contrast, during winter, the heating is opposite and the winds are directed out of the Asian continent. Thus, the wind stress in the Arabian Sea and Bay of Bengal is directed southwestward during winter and northwestward during summer (Schott and McCreary, 2001).

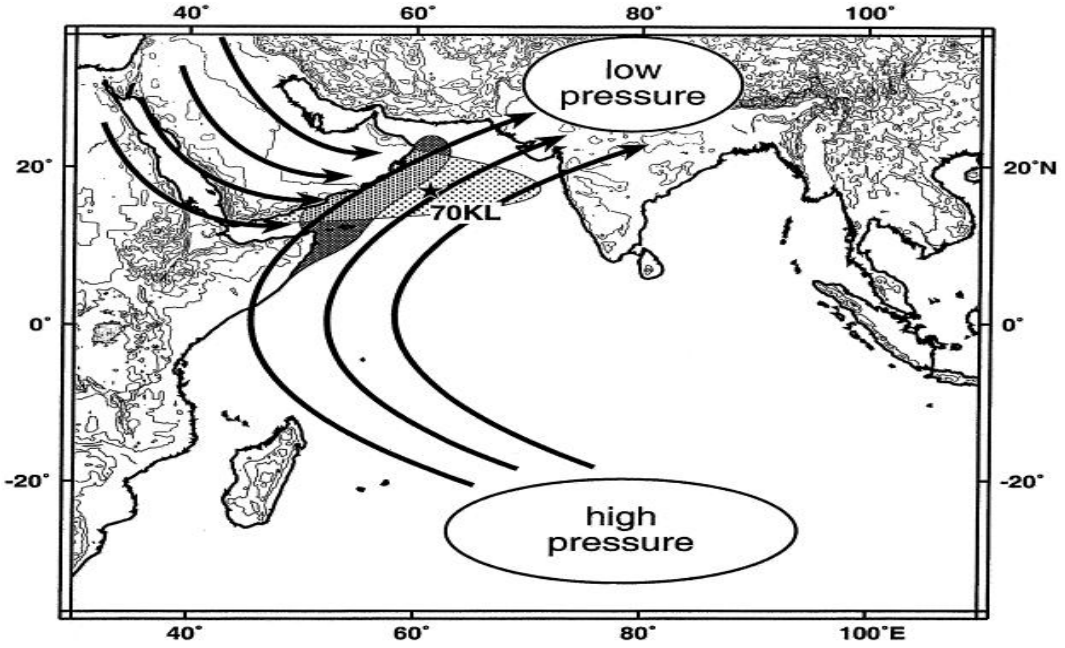

Figure 1.3: Pressure gradient generates Indian Ocean monsoon Clemens and Prell (1990).

1.3 Wave climate

The global wave height field varies seasonally. The highest waves are found at high latitudes, and the waves gradually decrease closer to the equator (Schott and McCreary, 2001). In the southern hemisphere of the Indian Ocean, wind speed and wave height are greater in southern winter than in summer. The long wave during the southern winter reflects the high propagation of southern Ocean swell into the Indian Ocean (Young and Babanin, 2006). In northern Indian Ocean, wind speed increases in mid of May and high winds continue until September. At Indian west coast shore, the significant wave height is up to 6 m through summer monsoon (Sabique et al., 2012).

1.4 Swells

Ocean swell studies are very important for many applications, such as coastal oceanographic studies, coastal management activities, and Ocean engineering (Sabique et al., 2012). Swells considered as surface waves that exceed their generating wind, and propagate across the ocean basins (Ardhuin et al., 2009). At other times waves of shorter wavelengths have been created locally, and travel through these waves. Such long waves are swells that have been generated and traveled far from their origin place. When swell interacts with the atmosphere, it loses some of its energy (Kudryavtsev and Makin, 2004). When the swell waves leave the storm area, their wave height decreases gradually,this might be due to the energy loss by air hindrance to steep waves, but also because the wave crests spread along a progressively wide front (Bearman et al., 1989). Recent surveys show that there are no consensus of the loss of swell energy (Collard et al., 2009). In deep water, the phase speed is proportional to wave period. Intense wind creates a longest wave periods which carry a significant amount of energy (Collard et al., 2009).

1.4.1 Swells in the Southern Indian Ocean

Satellite data revealed that there are three swells dominant zone in the tropical areas of pacific, Atlantic, and Indian Oceans. Strong wind blowing over the southern Indian Ocean creates high waves that propagate to the northern Indian Ocean (Sabique et al., 2012). The propagation of swell to the northern Indian ocean increases during the southern hemisphere winter (i.e., June – September). However, the Bay of Bengal and Arabian Sea have a high swell (between 0.5 m to 1.0 m) (Sabique et al., 2012).

1.5 Distribution of swell and wind-sea energy with frequency

The wind sea and the swell have been estimated by selecting the separation frequency to separate the wave spectrum into its wind-sea and swell parts. The spectra use these parts to calculate the significant wave height, peak period, mean direction of the wind-sea, and swell portions of the spectrum. Figure 1.4 shows the energy spectrum containing both swell and wind-sea. The swell has a narrow peak at low frequency, and the wind sea has a broader and higher peak at some of the higher frequencies. The swell and wind sea have been estimated by National Data Buoy Center (NDBC). The center have used the wave steepness method since 1997. This method assumes that wind-sea is steeper than the swell to determine a separation frequency. The maximum steepness (wave height divided by wave length) in the wave spectrum that occurs near the peak of wind-sea energy (Gilhousen and Hervey, 2001).

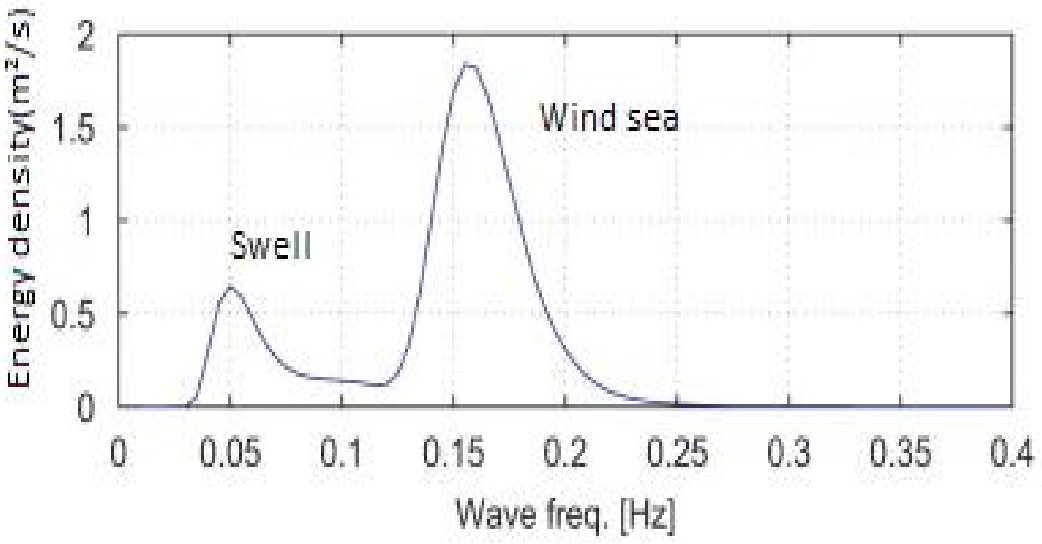

Figure 1.4: Wave spectrum shows the separation frequency and the distribution of swell and wind-seas energy with frequency.

Chapter 2

Data and Methods

2.1 Data

The data of the wave height, wave period, and the surface wind speed have been collected from seven grid point locations near shores in the northern Indian Ocean (see Figure 1.1). The wave height and the wave period values are combined to swell and wind sea. The total wave height is a square root of the sum of the squares of the separate trains:

$$H_{combined} = \sqrt{H_{swell}^2 + H_{wind}^2}. \tag{2.1}$$

The corresponding shore points (beaches) were selected because they represent different locations and different gentle beach slopes, except Maldives, which was assumed as an imaginary beach.

The dataset in this study were taken ERA-Interim, which is the latest global atmospheric re-analysis produced by the European Centre for Medium-Range Weather Forecasts (ECMWF) in collaboration with many institutions (ECMWF, 2006). The ERA-Interim software covers the period from 1 January 1989 to 31 December

2009 every six hour. The analysis provides the global surface wind, and the two wave parameters significant height and peak period (Kulseng, 2010).

The ERA-40 software is carried out by ECMWF with the goal of producing the best probable set of analyses, given the varying observing system and the available computational resources (Uppala et al., 2005). This re-analysis is the first model in which an ocean wave prediction model is coupled with an atmospheric model. Furthermore, its a final product consists of the longest and most complete obtainable global wave dataset. It uses spherical coordinates given as 1.5° by 1.5° latitude-longitude grid resolution, covering the whole globe (Semedo et al., 2009). The horizontal resolution of the wave model in ERA-Interim is 110 km (Dee et al., 2011).

ECMWF uses the global Wave Model WAM model to calculate wave spectra in two dimensions, which uses non-stationary and non-homogeneous wind fields in forecasting wind waves (Al-Salem et al., 2005). The WAM is forced by surface winds using the wave energy balance equations to calculate the evolution in time and space of each component of the wave spectrum for selected frequency bands and direction bins. The frequency bands cover the total spectra of wind sea and swell, and the direction bins cover the total circle. The WAM model includes the following physical processes: Wind-wave interaction, wave-wave interaction, dissipation and shallow-water bottom dissipation (the bottom friction) (Caires and Sterl, 2005).

2.2 Theory

2.2.1 Wave runup equations

Stochdon et al. (2006) empirical equations are the best relationships driven from field observations of wave height, wave length, and runup. These equations are widely used in engineering computation of the physical processing-based approach (Vitousek et al., 2010).

Table 2.1: Name of beaches locations, its latitude and longitude, the slope of the beaches, the directions of the beaches, model grid point position (latitude and longitude), the corresponding wave forecasting distance from grid points to the beaches, and direction from beaches to the grid points, this table contain for all location except Maldives beach is just an imaginary beach.

Location	Lat/Long beach	Beach slope	Exposure	Lat/long grid points	Distance km	Direction to grid point
Oman	18°41′57″ 56°45′08″	0.23	E	18.5N 57.0E	34	SE
Somalia	5°23′12″ 48°33′35″	0.46	E	05.0N 49.0E	65	SE
Sri Lanka	7°47′16″ 81°38′37″	0.23	NE	8.0N 81.5E	28	NW
Goa	15°14′34″ 73°55′21″	2.30	W	14.5N 74.0E	82	S
India	19°53′11″ 72°40′54″	2.30	W	20.0N 72.5E	22	NW
Pakistan	25°28′03″ 66°18′02″	0.29	S	25.0N 66.0E	60	SSW

The ratio(ξ) between the beach slope β and the wave steepness $\sqrt{\frac{H_\circ}{L_\circ}}$ is called Iribarren number and it is given by,

$$\xi = \frac{\tan\beta}{\sqrt{\frac{H_\circ}{L_\circ}}}, \tag{2.2}$$

where $H_\circ$ is the wave height in deep water, and $L_\circ$ is the wave length in deep water, which is calculated by,

$$L_\circ = \frac{gT^2}{2\pi}, \tag{2.3}$$

where g is the gravity acceleration and T is the time. Iribarren and Nogales who were the first that used these parameters to determine which type of wave breaking occurs, ξ also describes how the waves break (Battjes, 1974). Low Iribarren number indicates dissipative situation, while high numbers indicate more reflective surf zones (Ruggiero et al., 2004).

Basic relationships of extreme runup, setup, and significant swash (which combine incidence and infragravity motion), are given by,

$$R_2 =< \eta > +\frac{S}{2}, \tag{2.4}$$

where R_2 is the extreme wave runup, $< \eta >$ is the wave set up, and $S = (S_{inc}^2 + S_{IG}^2)^{\frac{1}{2}}$ is the significant swash, which is defined by the square root of the incidence wave when $T < 20$ s, S_{inc}^2, and the infragravity wave when $T > 20$ s, S_{IG}^2. The extreme wave runup is a function of $f(H_\circ, T, \beta)$, and therefor it is a function of $g(< \eta >, S_{inc}, S_{IG})$. The incident and infragravity swash are given by

$$S_{inc} = 0.75\beta\sqrt{\frac{H_\circ}{L_\circ}} S_{inc} = 0.06\sqrt{\frac{H_\circ}{L_\circ}} \tag{2.5}$$

A better linear relation that combines $< \eta > +S/2$ and R_2 has been drived from Stochdon et al. (2006) experiement. Then the Equation (2.4) becomes

$$R_2 = 1.1\left(< \eta > +\frac{S}{2}\right). \tag{2.6}$$

The general formula for calculating the non-dissipative runup can be written as

$$R_2 = 1.1\left(0.35\beta\left[H_\circ L_\circ\right]^{\frac{1}{2}} + \frac{\left[H_\circ L_\circ\left(0.56\beta^2 + 0.004\right)\right]^{\frac{1}{2}}}{2}\right). \tag{2.7}$$

When the beach slope $\beta < 0.1$, the runup is independent of β, and it is proportional to $(H_\circ L_\circ)^{\frac{1}{2}}$. When $\xi < 0.3$, the dissipative runup is calculated by,

$$R_2 = 0.043\left(H_\circ L_\circ\right)^{\frac{1}{2}}. \tag{2.8}$$

2.3 Methods

2.3.1 The wave energy-balance equation

Wave forecasting is estimation of transfer of energy from the wind to surface waves. Three processes considered as sources S of wave energy: The wave wind generation, S_{in}, the dissipation loss due to breaking wave and other causes, S_{dis} and four-wave interactions, S_{nl} (Janssen, 2008). In other words,

$$S = S_{in} + S_{nl} + S_{dis}. \tag{2.9}$$

In deep water, we assume that the curent is neglected, then the wave energy conservation equation takes the form:

$$\frac{\partial f}{\partial t} + Cg\nabla F = S_{in} + S_{nl} + S_{dis}, \tag{2.10}$$

where $F = F(k; x, t)$ is a two dimensional wave energy spectrum function of the space direction and the time. The wave energy travels with the group velocity Cg (Komen et al., 1984). The dispersion waves in deep water, the group velocity (cg) is only half of the phase speed (Laing et al., 1998).

2.3.2 Wind Input

In recent years, researchers are working on the wave forcasting using energy spectrum begin to understand how energy transfers from wind to surface waves (Moskowitz, 1964). Mechanical energy input by wind stress is very important for the energetics of the global ocean (Wang and Huang, 2004). The wind is considered as the only source of energy input to the sea surface over time-scale (Laing et al., 1998). The wind input to the surface waves is given as,

$$S_{in} = A(f, \theta) + B(f, \theta)E(f, \theta). \tag{2.11}$$

In Equation (2.11), Phillips (1957) suggested that the first term on the right hand, which is the frictional force due to the interaction between waves and turbulent pressure patterns in the air. Miles (1957) suggested the second term, which represents the feedback between induced turbulent pressure patterns and growing waves.

2.3.3 Dissipation of swell energy

The dissipation that produced from swell is a significant term in the wave energy balance at large scales (Ardhuin et al., 2009). This term is the sum of lost occurs by three different processes: White-capping, wave-bottom interaction and surface breaking (Laing et al., 1998). The estimation of the wave field depends on the time t, latitude ϕ and longitude L. This estimeation is described by a two dimension spectral density function, $G(f, \theta)$ where f is the frequency and θ is the direction(Collard et al., 2009). The spectral density is created in the spreading of group speed Cg, which can be described as a function of G at any initial time $t_\circ$, see Figure 2.1.

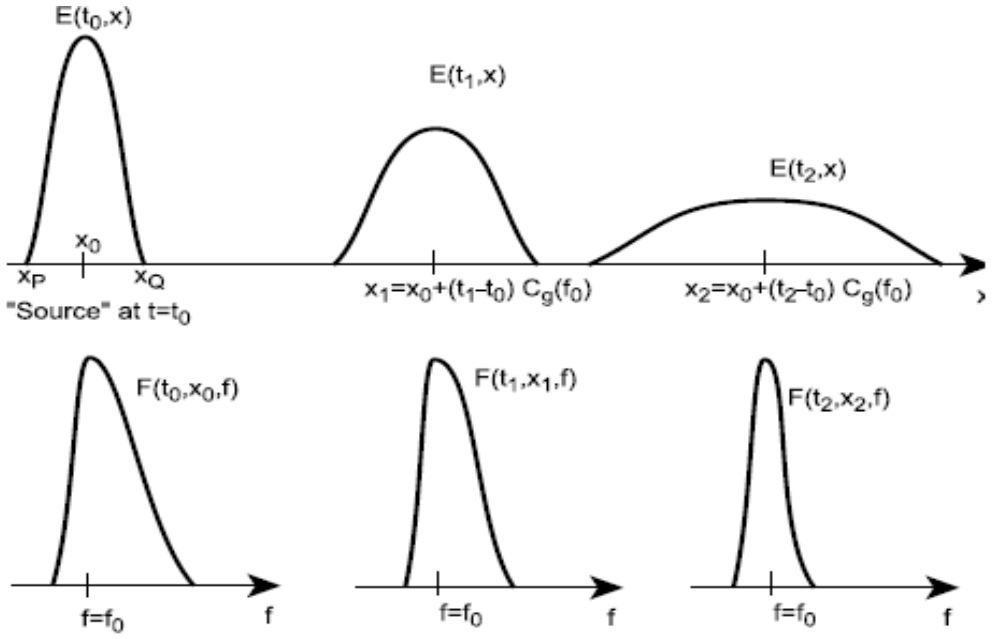

Figure 2.1: Distribution of swell waves in one dimension. At any given time the spectrum is given by a propagation of the spectra at $t = t_\circ$
from (Collard et al., 2009).

This function permits for a spatial decay, then the equation of the spectral energy balance in deep water can be written as:

$$G(t, \phi, L, f, \theta) = G(t_\circ, \phi_\circ, L_\circ, f, \theta_\circ) \exp\left(\int_{t_\circ}^{t} -\mu C g dt\right). \tag{2.12}$$

where we assumed that: There is no current motion at the surface, the initial position is $\phi_\circ$ and the direction is $\theta_\circ$ (μ is the decay rate)(Collard et al., 2009).

Chapter 3

Results

In this section, we will present the results obtained for the frequency distributions of wave runup for all years, and give details of the common values of runup. The scatter plots of wave runup, wave length and wave height illustrate two peaks of wind (short wave length and high wave height), and swell (long wave length and low wave height). Relationships between wave runup, wave height, and wind speed demonstrate that in most cases maximum runup and wave height are proportional to wind speed. Wave height, runup and wind speed values are varying with time of the year due to variation of monsoon.

3.1 Frequency distribution of runup

The frequency distribution of the estimated runup at the shore in Oman (Figure 3.1a) reveals that in 49% of the cases the runup is between 0.5m and 1.0m, while the highest number of cases of wave runup at the shore in Somalia, 66%, occurs between 0.5m and 1.0m (look Figure 3.1b). At Sri Lanka's shore, Figure 4.1c shows that most cases, 52%, wave runup is less than 0.5m. The estimation of wave runup at the shore in Goa (Figure 3.1d) reveals that 71% occur between 0.5 and 1.0m. At the shore in India, Figure 3.1e, most number of cases, 59%, runup is less than 0.5m. While at the shore in Pakistan, Figure 3.1f shows that 53% of the cases runup is between 0.5 and 1.0m. Figures 3.1g1 and 3.1g2 demonstrate that at

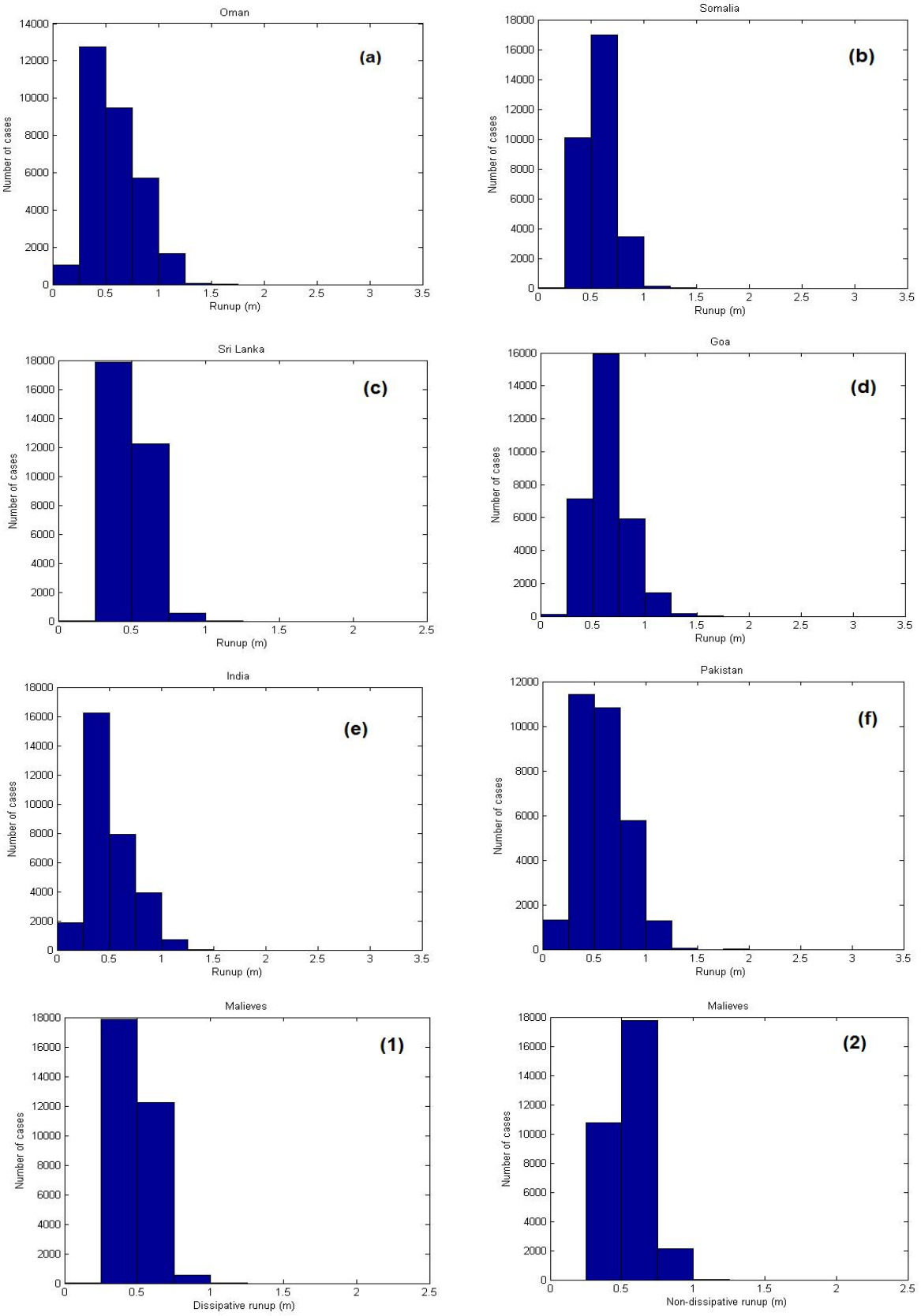

Figure 3.1: Histogram of runup (m) at the shore in (a) Oman (b) Somalia (c) Sri Lanka (d) Goa. Histogram of runup (m) at the shore in (e) India (f) Pakistan. Histogram of runup (m) at the shore in Maldives: (1) Dissipative runup and (2) Non-dissipative runup.

an imaginary dissipative beach when Iribarren number $\xi < 0.3$ in Maldives 58% of the cases runup is less than 0.5m, while on a non-dissipative beach with Iribarren number must equal to 0.3. 57.8% of the cases runup between 0.5 and 1.0m.

Summary

The highest number of cases of estimated wave runup lies between 0.5m and 1.0m for all locations except Sri Lanka, Indian and Maldives (dissipative runup) shores where it is less than 0.5m (see Figures 3.1e and 3.1g).

3.2 Wave height versus wind speed

The wave height forecast at the Oman model grid point (see Table 2.1) is compared to the wind speed at that point. A scatter plot of wave height versus wind speed is shown in Figure 3.2a generally, a weak wind creates small waves, while a strong wind creates high waves (see the inserted curve for fully developed wind sea). But here the scatter is quite large, revealing effects of swell (large wave height, low wind speed), and fetch limitation (high wind speed, small wave height). At the Somalia grid point (Figure 3.2b), for wind speeds less than 8 ms^{-1} swell is more prominent than wind sea. There is a much closer relation between wave height and wind speed at the Somalia's grid points than at the Oman grid point (compare Figure 3.2a with Figure 3.2b). At Sri Lanka grid pint, (Figure 3.2c), for wind speeds smaller than 8 ms^{-1} swell more than wind speed affects wave height. In Goa's shore, Figure 3.2d shows that the highest waves occur due to the wind sea, and low waves which are independent of the changing of wind speed. On India's shore the strongest wind speed generate the highest wave height, wind less than $10ms^{-1}$, swell more affect of wave height than wind sea, see Figure 3.2e). The similarity between the Goa and India grid points lies in: Their highest wave height depend of strong wind more than swell. Mostly the swell it has a far greater impact of wave height than wind speed (compare Figures 3.2d and 3.2e). At the Pakistan's grid points, Figure 3.2f shows that the wave height depends on wind speed when

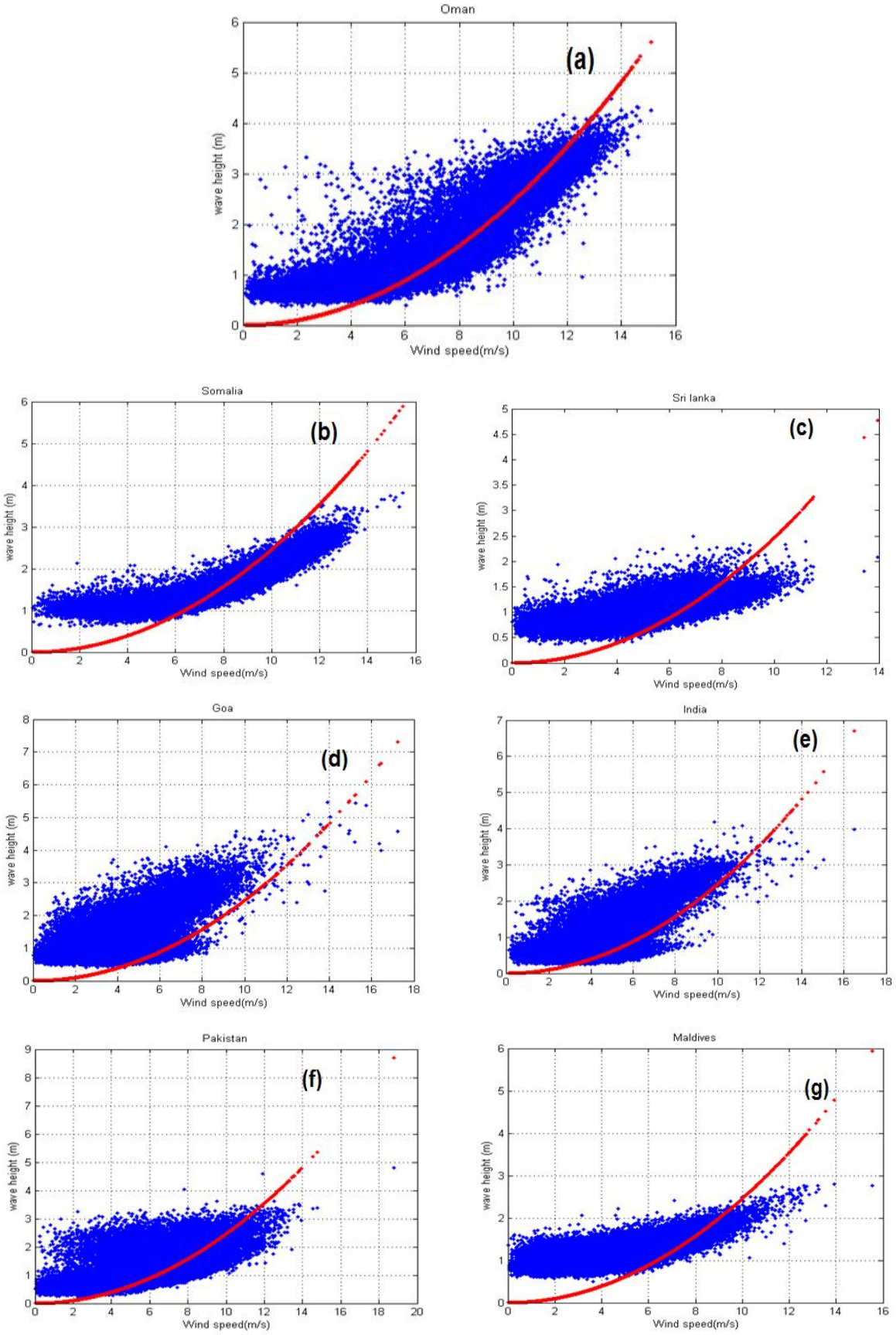

Figure 3.2: Relationship between wave height and wind speed. Fully developed wind sea is represented the inserted red curve at the grid point in (a) Oman (b) Somalia (c) Sri Lanka (d) Goa. Relationship between wave height and wind speed. Fully developed wind sea is represented the inserted red curve at the grid point in (e) India (f) Pakistan (g) Maldives.

it is stronger than 9ms^{-1}, but less than 9ms^{-1} wave height is dominated by swell. On the Maldives, Figure 3.2g suggests that for wind speeds less than 6 ms^{-1} swell is dominant.

Summary

The highest values of wave height occur in locations that are situated at high latitude (Pakistan, Oman, Goa and India). Generally a weak wind creates small waves, while a strong wind creates high waves. As most cases lie above the curve for fully developed wind sea, swell is more dominant than wind sea.

3.3 Runup versus wind speed

At Oman's shore the mean value of runup is 0.58m, some of the extreme values of wave runup occur at weak wind speed, hence they are due to swell (see Figure 3.3a). Extreme values of wave runup at high wind speed are also seen. At the shore in Somalia the mean value of runup is 0.57m, Figure 3.3b shows that extreme wave runup occurs at mid wind speed from 4 ms^{-1} to 12 ms^{-1}. At Sri Lanka shore the mean value is 0.52m, the extreme values of wave runup occurs due to swell as shown in Figure 3.3c, also, the strong wind speed has no impact of the wave runup. Figure 3.3d shows Goa shore runup and its mean value is 0.64m. It is the highest for all locations, high wave runup dependent of strong wind speed. At Indian shore (Figure 3.3e) the highest values of runup occur at mid and stronger wind speeds. Figures 3.3f) and3.3g shows Pakistan and Maldives shore, most of the extreme runup doesn't occur at strong wind speed which indicates effect of swell.

Summary

In most locations, the largest wave runup is generated at medium values of the wind speed. The strongest wind doesn't generate maximum runup. This indicates

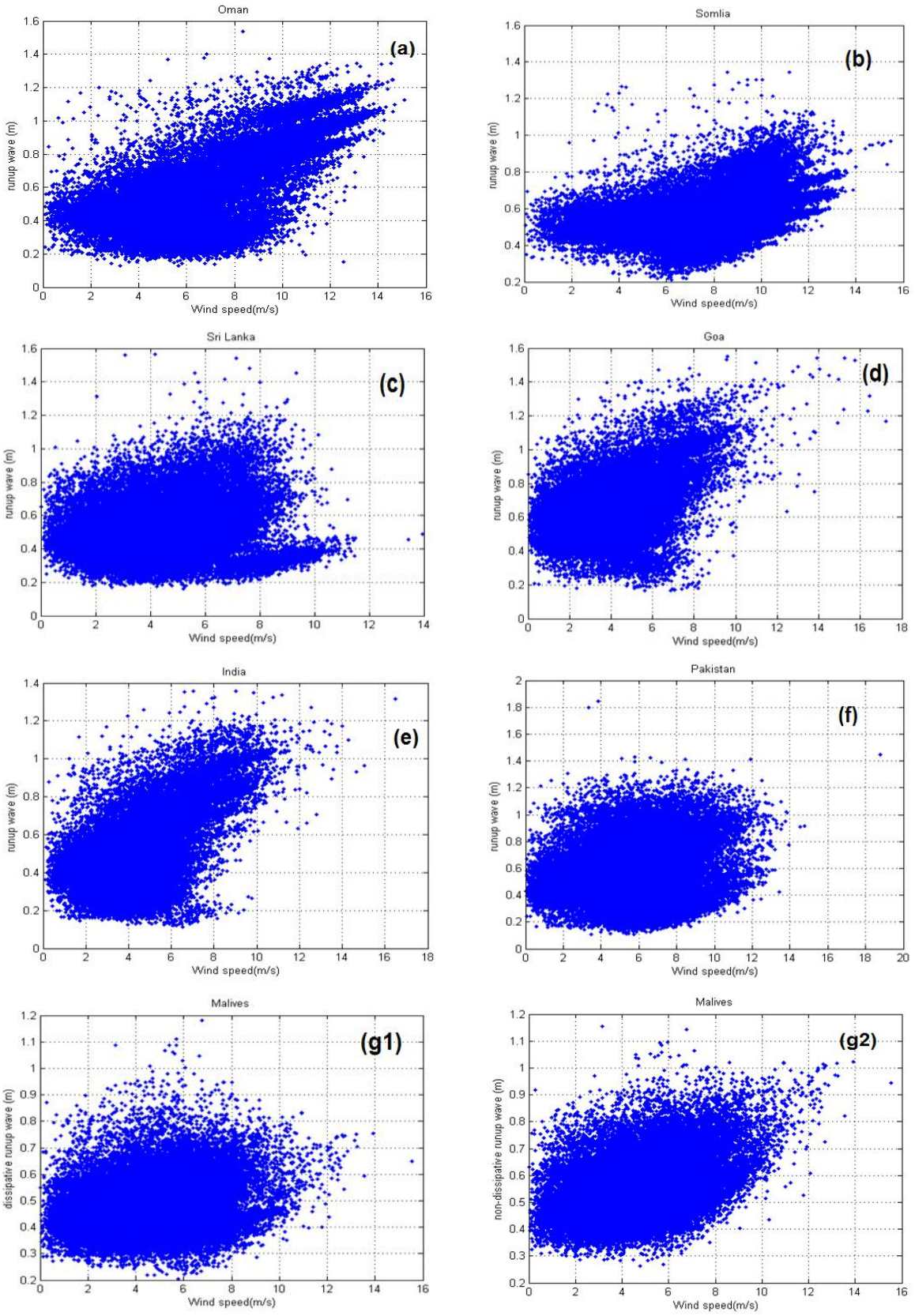

Figure 3.3: Runup versus wind speed at the shore in (a) Oman (b) Somalia (c) Sri Lanka (d) Goa. Runup versus wind speed at the shore in (e) India (f) Pakistan. Runup versus wind speed on the Maldives (g1) dissipative wave runup (g2) Non-dissipative wave runup.

that swell strongly contributes to generate extreme runup. The highest mean value of runup is 0.64m, and occurs at the shore in Goa; while the lowest is 0.49m and occurs at the shore on the Maldives. The mean value of runup for all locations is 0.56m.

3.4 Runup as a function of wave height and wave length

Figure 3.4a shows the runup as a function of wave length and wave height at the shore in Oman. Runup more than 1.25 m is produced by wind waves with heights between 3.5 to 4.5 m and wave lengths between 200 to 300m. Values more than 1.25 m also occur for swell with height 2.0 m and wave lengths longer than 500 m. The maximum runup value (> 1.5 m) is generated by a long swell of about 600 m. In Figure 3.4b At Somalia's shore runup more than 1.0 m is generated by wind waves with wave heights between 2.5 to 3.5 m and wave lengths between 150 to 250m.

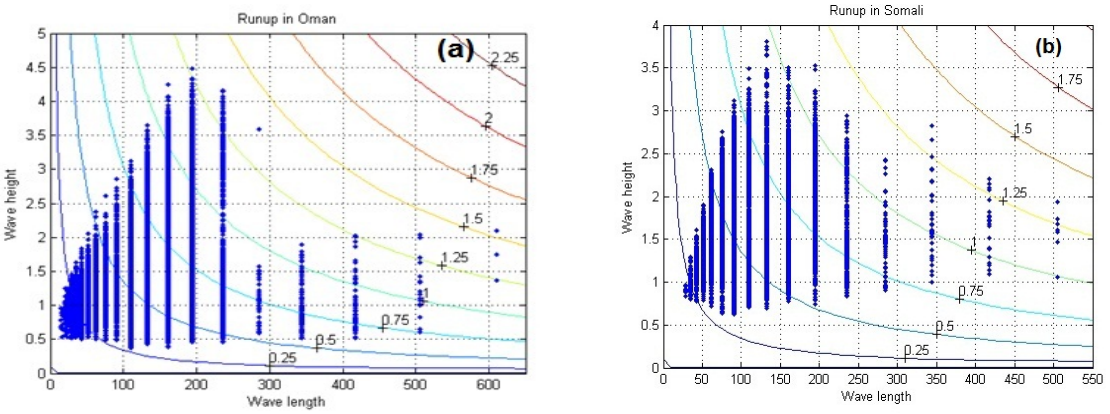

Figure 3.4: Wave runup as a function of wave height and wave length at: (a) Oman, (b) Somalia. The contour lines are given by the runup formula for dissipative beaches.

Runup more than 1.0 m occurs for swell with wave heights around 2.0 m and wave lengths longer than 280 m. Ten cases of extreme runup larger than 1.25 m occur for swell waves longer than 340 m. At Sri Lanka's shore, Figure 3.5c shows two cases of extreme wave runup larger than 1.5m which occurs at long wave length,

most of the extreme wave runup occurs for swell between 500m to 800m wave length. At Goa's shore, in Figure 3.5d runup more than 1.5 m is produced by wind waves for high wave heights between 4.0 to 6.0 m and wave lengths between 200 to 300m.

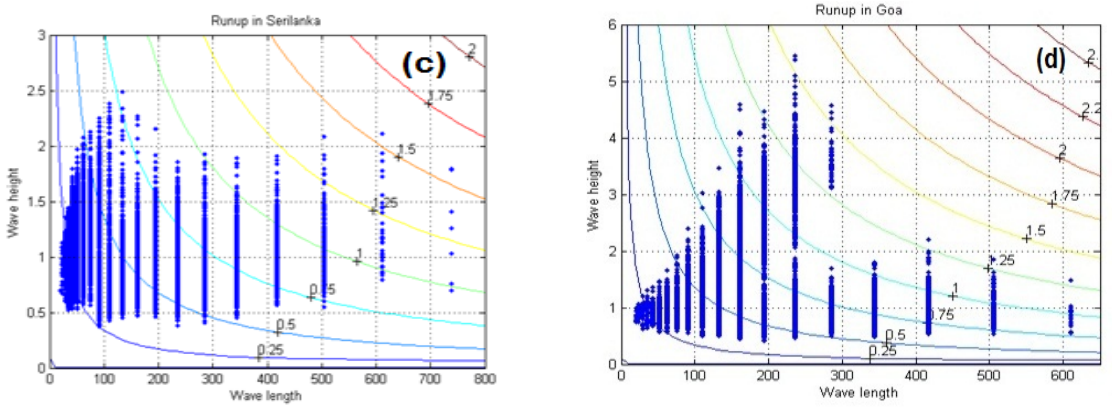

Figure 3.5: Wave runup as a function of wave height and wave length at: (c) Sri Lanka, (d) Goa. The contour lines are given by the runup formula for dissipative beaches.

The extreme values of wave runup are only at high wave height and medium wave length and therefore due to wind. Figure 3.6e at Indian shore, runup more than 1.25 m occurs with wind waves for high wave height between 3.0 to 4.5 m and wave lengths between 200 to 300m. Runup more than 0.75m occurs for swell with wave heights between 0.5 to 1.0 m, and wave lengths between 400 to 600m. Figure 3.6f shows, at the shore in Pakistan, two cases of the extreme values of wave runup more than 1.75m at swell waves longer than 700m. At Maldives shore Figure 3.7g present the dissipative runup is dependent of long swell wave more than wind speed.

Summary

Generally the extreme runup is generated by swell of long wave lengths. The highest wave height doesn't affect the extreme runup. Locations at high latitude: Oman, Goa and Pakistan (see Figures 3.4a, 3.5d and 3.6f) have higher wave heights than the other locations due to the monsoon.

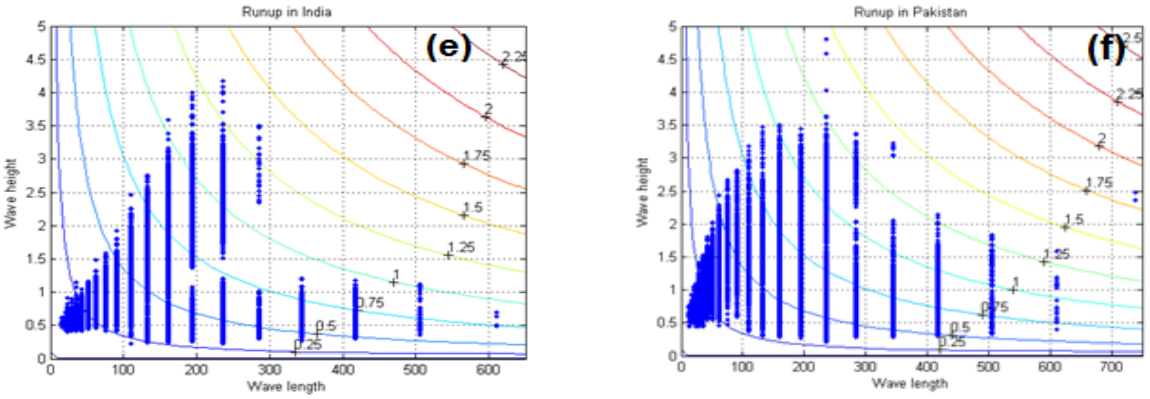

Figure 3.6: Wave runup as a function of wave height and wave length at: (e) India, (f) Pakistan. The contour lines are given by the runup formula for dissipative beaches.

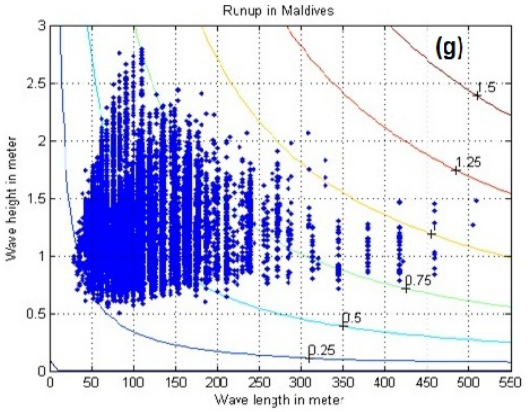

Figure 3.7: Wave runup as a function of wave height and wave length at Maldievs. The contour lines are given by the runup formula for dissipative beaches.

3.5 Seasonal variation of runup, wave height and wind speed

By finding the monthly mean values of the wind speed, wave height and estimated runup, we can study their seasonal variation. On the shore in Oman Figure 3.7a shows that the lowest monthly mean values of runup (< 0.4 m) are occur between December and February, while the highest values (> 0.9 m) are occur in July.

The highest monthly mean values of wave height 3m are occur in July, and the lowest mean values are occur between December and February. In general, wave runup increases when the wave height increases and the wave height depend more

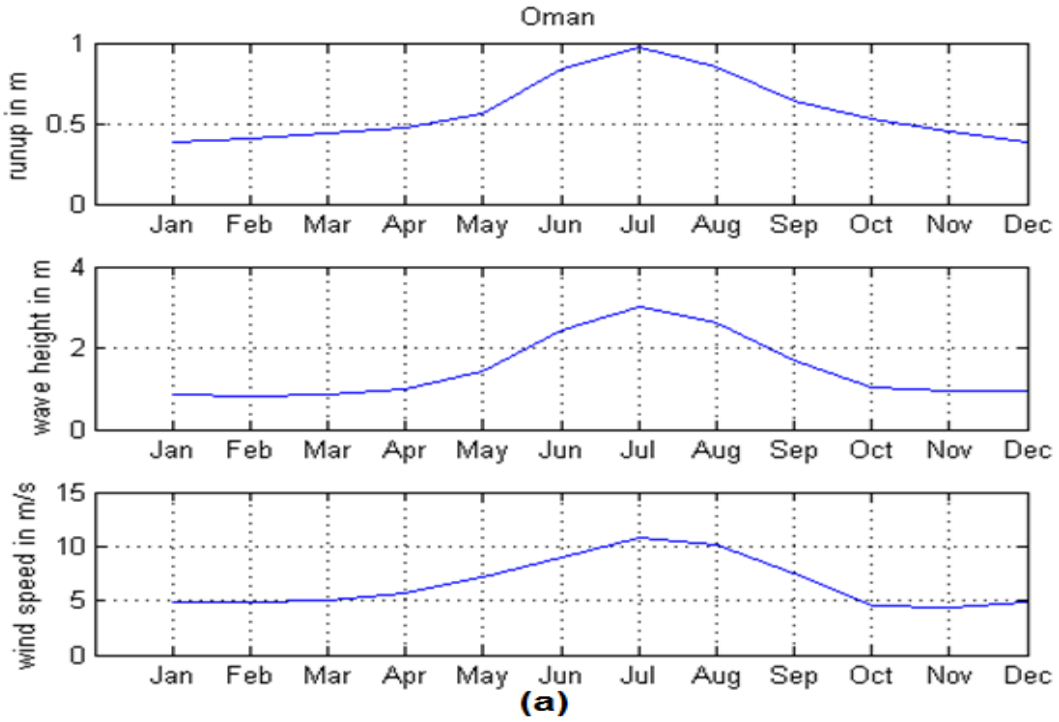

Figure 3.7a: Seasonal variation of wind speed, wave height and runup at Oman.

strongly on wind speed than runup does. In Somalia's shore in Figure 3.7b the lowest monthly mean values of wave height (< 1.2m) are occur due to weakest wind ($< 5\text{ms}^{-1}$) in April, whereas the lowest monthly mean values of runup are occur between December and March, and seems not to depend of wave height to that same degree.

There are two peaks of wave height: One small peak occurs during winter monsoon between November and April, the large peak occurs during the summer monsoon between April and October. During the absence of the summer monsoon the runup depends of long wave length swell. The highest values produced due to the composite influence of wind sea and swell occur in July. On the shore of Sri Lanka (Figure 3.7c), the highest monthly mean values of runup is (> 0.6), while the highest monthly mean values of wave height (< 1.2m).

The lowest values of monthly mean runup are 0.4m occur between February and January. At the shore in Goa (Figure 3.7d) the highest monthly mean values of wave height are $\approx$2.6m occur at the strongest wind speed ($> 6\text{ms}^{-1}$) in July, and the lowest values (< 0.8m) occur between December and January while the

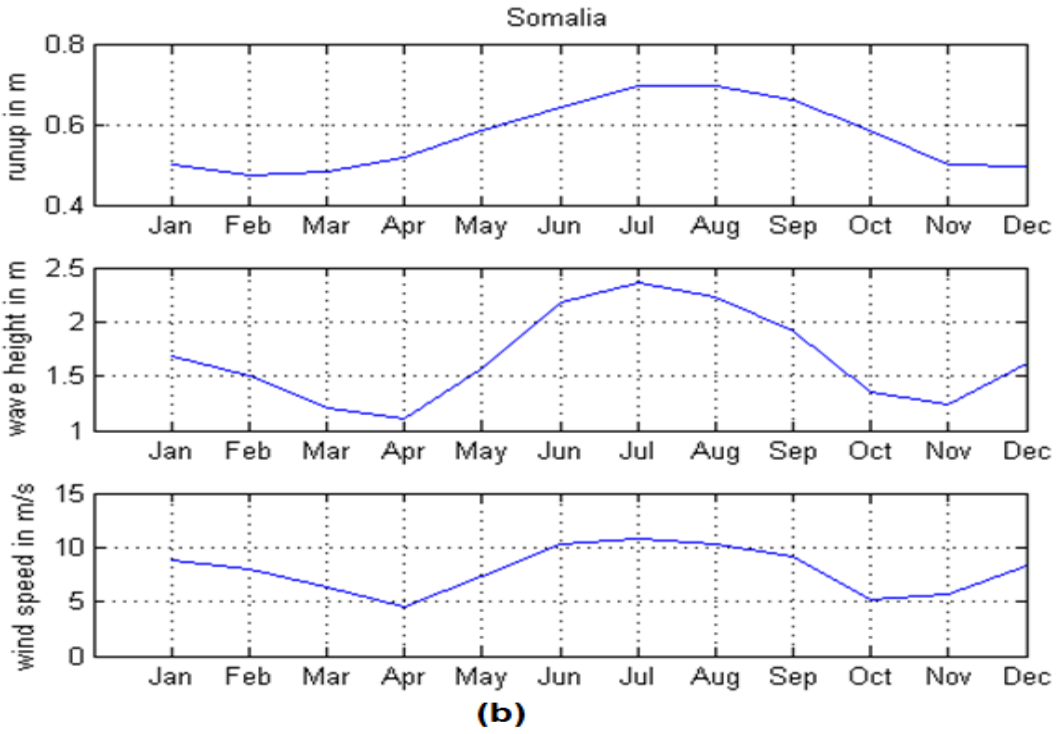

Figure 3.7b: Seasonal variation of wind speed, wave height and runup at Somalia.

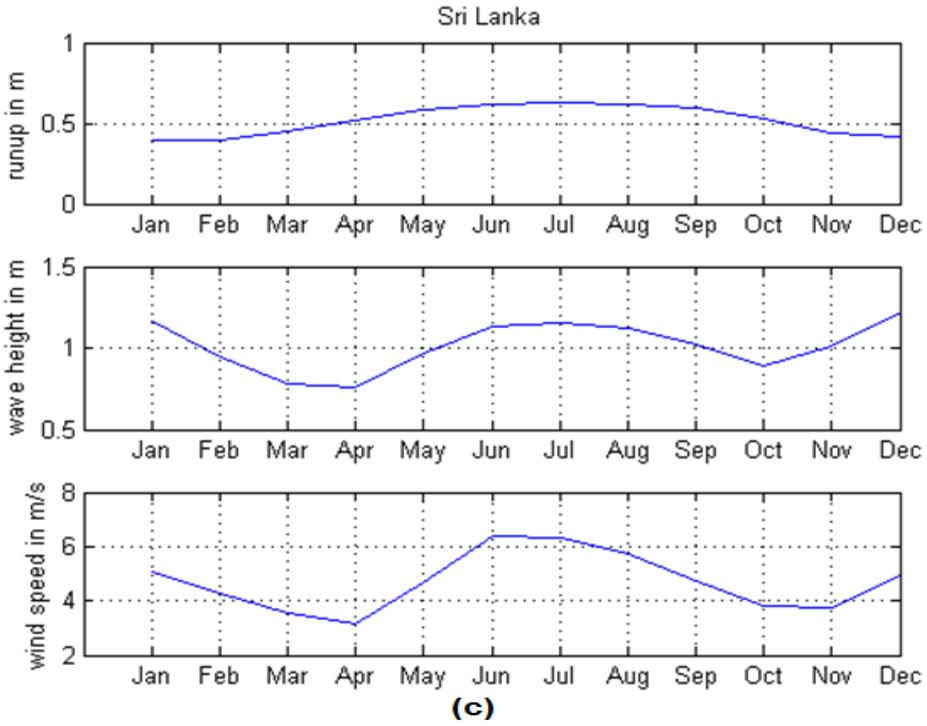

Figure 3.7c: Seasonal variation of wind speed, wave height and runup at Sri Lanka.

weakest wind speed is occurs in October. The highest monthly mean values of runup are 0.9m occur in July during the summer monsoon, whilst lowest values of runup are 0.5m occur in January during winter monsoon.

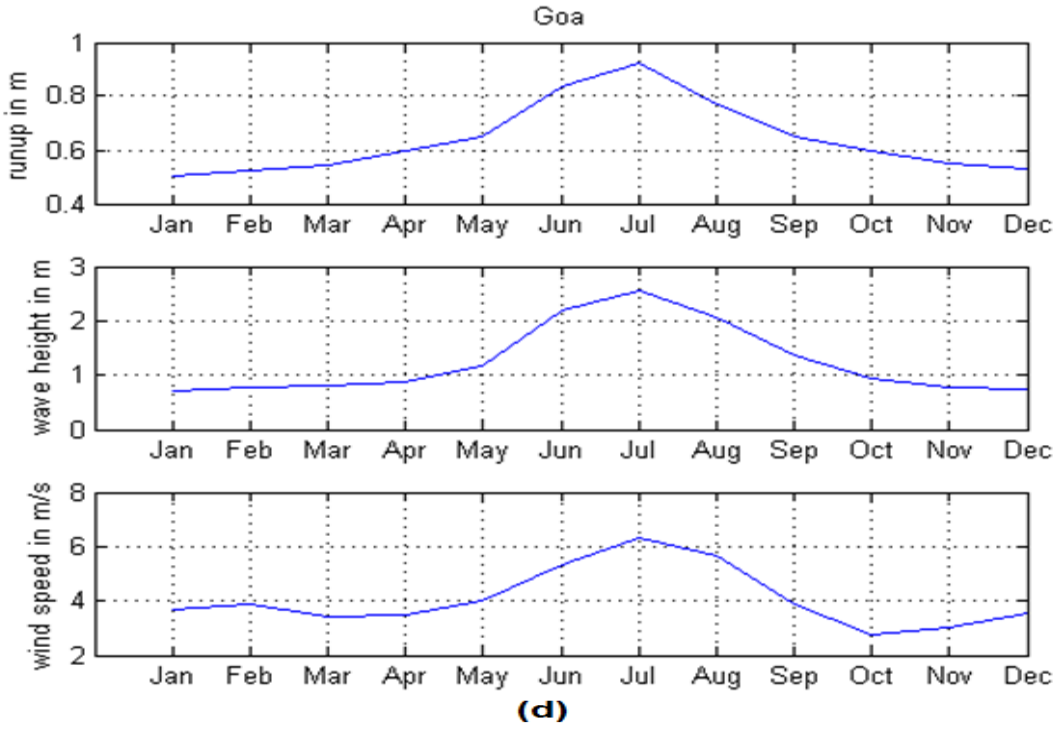

Figure 3.7d: Seasonal variation of wind speed, wave height and runup at Goa.

In Indian's shore (Figure 3.7e) the lowest monthly mean values of wave height are occur from December to January, about 0.4m, while the highest values are ≈2.2m occur in July. The wave runup and wave height increase and decrease gradually with repect to time. The wave height and runup are not depending on wind speed during October, November and December, which indicates that the swell is more dominant than wind sea.The lowest monthly mean values of runup are 0.4m, which occur from December to April, The highest values are ≈0.9m occurs together with the strongest wave height in July.

At the shore in Pakistan (Figure 3.7f) the highest monthly mean values of wave height and runup are 2.4 and 0.95m, respectively, in July. The highest wind speed 7.5 ms^{-1} occurs between May and June, but stays relatively high the rest of the summer. Lowest monthly mean values of wave height 0.6m and runup 0.4m occur

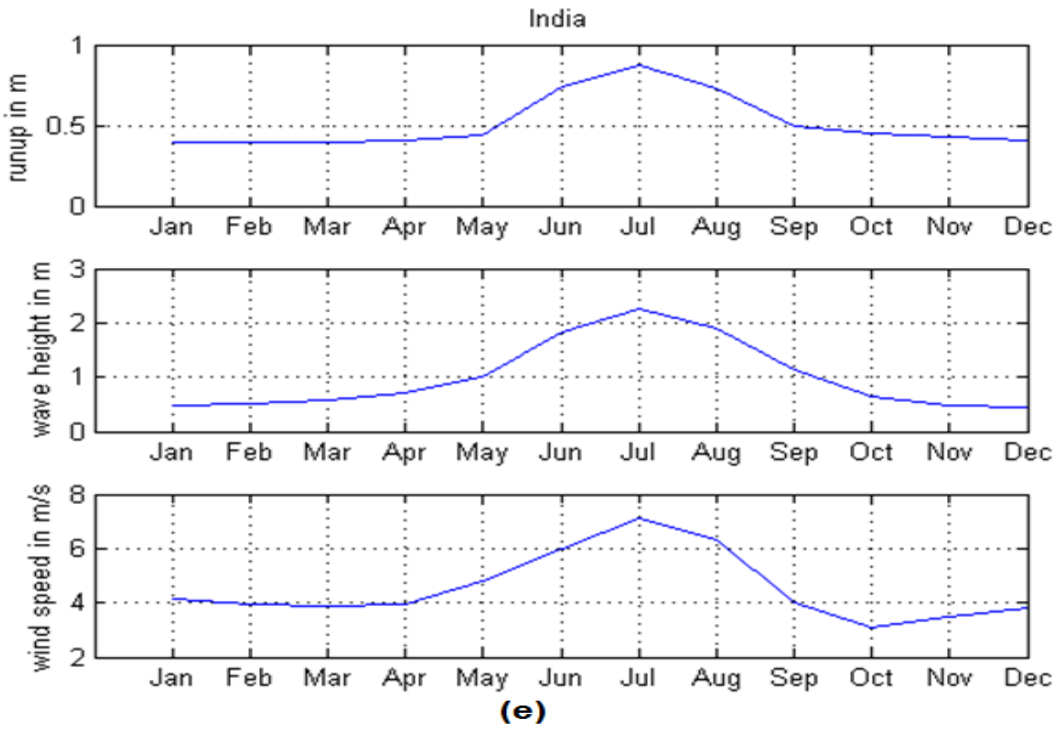

Figure 3.7e: Seasonal variation of wind speed, wave height and runup at India.

between December and January, while the weakest wind speed (< 3.5m) occur during November and December.

In Maldives shore (Figure 3.7g) the highest monthly mean values of wave height (1.5m) and runup (0.6m) occur in July, whereas the strongest wind speed (> 5.5m) in May and June. The lowest monthly mean values of runup (> 0.4m) occur between January and February, while the lowest values of wave height (0.9m) occur in March at the weakest wind speed.

Summary

The highest values of runup in most locations occur at the highest wave height in summer monsoon in July due to composite swell and wind sea, while the lowest occur in January and December due to swell.

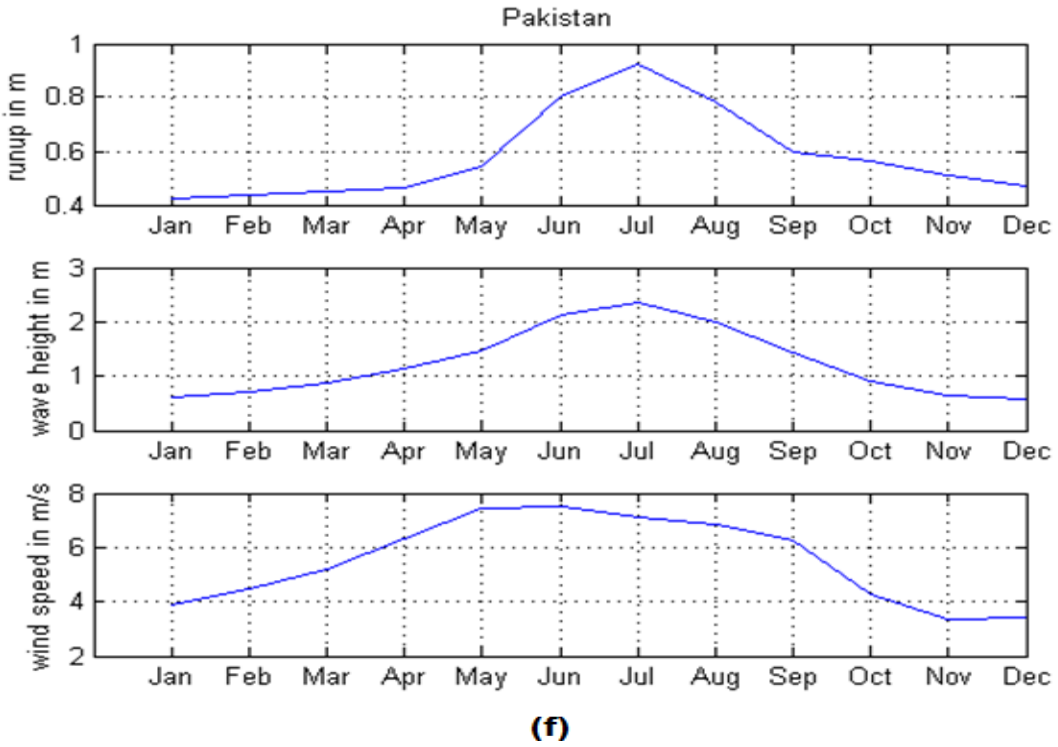

Figure 3.7f: Seasonal variation of wind speed, wave height and runup at Pakistan.

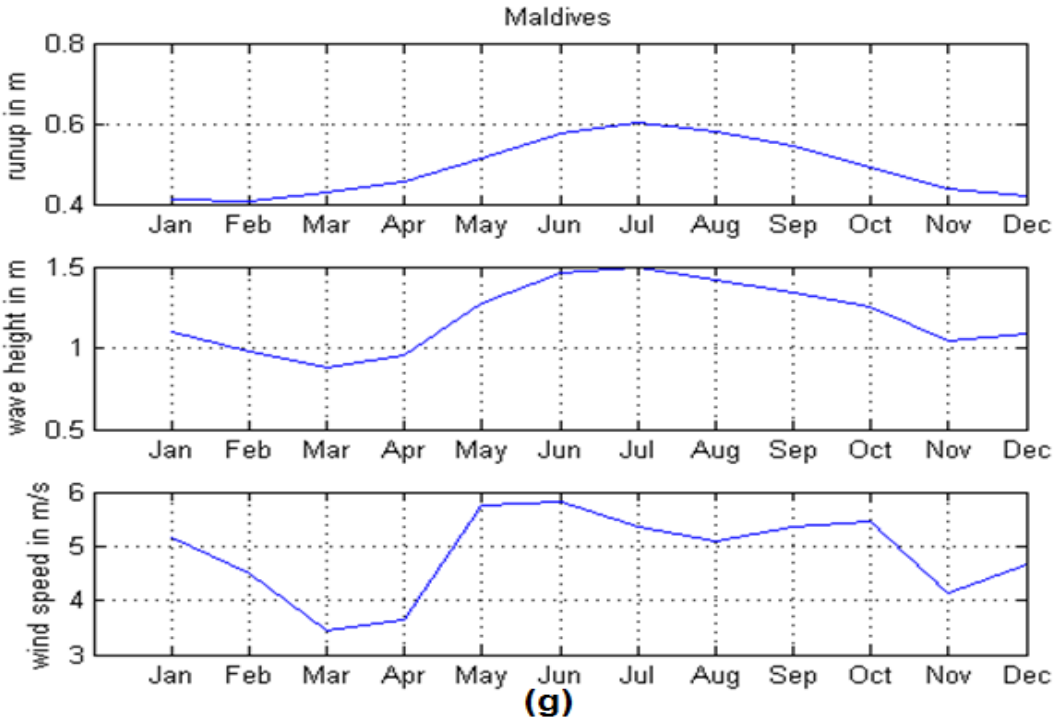

Figure 3.7g: Seasonal variation of wind speed, wave height and runup at Maldives.

Chapter 4

Discussion

The frequency distributions to estimated wave runup at the shores reveal that more than half of the time runup is between than 0.5–0.75m. Regarding wind speed effects of wave height, generally we know that a weak wind creates low wave height and a strong wind creates high wave height. Most of cases lie above the curve for fully developed wind sea, are dominant by swell more than wind sea. Wave height values become higher at high latitudes (Oman, Pakistan, and Goa) and decrease towards the Equator (Sri Lanka, Maldives and Somalia). Generally speaking, the highest runup generate at medium wind speed. This suggested that swell strongly contributes to generate extreme runup.

During the rest of pre-monsoon, the swell is a dominant factor in determining the wave height and runup of the Northern Indian Ocean. Always the maximum wave runup and wave height occurs on summer monsoon specially in July. That is due to the wind blowing from the Indian Ocean to the Asian continent. Low wave runup occurs during the weak winter monsoon. The extreme runup waves are generated due to swell, besides the influence of the southwest summer monsoon winds at all locations with the exception of Goa and India which are affected by wind more than swell. The maximum runup is found in Pakistan, which greater than 1.75m due to swell, the lowest values in Maldives. The longest swell wave

(more than 700m) occurs at the shore in Sri Lanka, whilst the lowest swell is (≈500m) takes place at the shores in Maldives and Somalia.

However the northern Indian Ocean is strongly affected by swell coming from southern Indian Ocean beside influence of the wind in summer monsoon. Swell increased during the southern hemisphere winter (June, July, August and September).

The highest mean values of runup occur at the shore in Goa 0.64m, where the high wave runup depends on strong wind speed. Wave height depends entirely on wind speed at the shores in Somalia and Sri Lanka (Figure 3.7b and Figure 3.7f). The special case at an imaginary beach on Maldives, where the highest dissipative runup seems to be affected by swell more than wind, while non-dissipative runup becomes more influenced by strong wind speed. The highest frequent distribution of non dissipative runup is 57.8%, which occurs between 1.0 and 0.5 m, while 58.1% of dissipative runup occurs when less than 0.5 m. The mean values of non dissipative runup are 0.56 m, which are greater than the mean values of dissipative runup (0.49 m). This indicates that the runup increases when beach slopes increase (when the Iribarren number is equal or greater than 0.3).

The methods which we used contain some uncertainty because: We don't involve the wind direction, we just assumed that the wave height and the period at the grid points are the same at the beach. We also neglected the tidal effect. We assumed that the slope is not changing from sea to the beach. We took the imaginary beach slope in Maldives at two cases investigating two conditions: Dissipative when Iribarren number is less than 0.3, while on a non-dissipative beach with Iribarren number must equal to 0.3.

Chapter 5

Conclusion and recommendations

The estimation of runup on natural beaches was carried out for seven locations in northern Indian Ocean covers the period from 1 January 1989 to 31 December 2009 every six hour. The most highest frequent distribution to estimated wave runup occurs between 1.0 and 0.5 m. In general, the wave runup is dominant by swell more than wind sea. The wave height depends on locations, where it is increases at high latitude and decreases towards the Equator. The maximum runup and wave height are occur in summer wind monsoon besides the influence of swell coming from southern Indian Ocean during the southern hemisphere winter. However, run up values are affected by swell, wind monsoon and beach slopes (when Iribarren number is equal or greater than 0.3). We can propose some recommendations needed in order to get more reliable results:

- Using the information on wind direction and the fetch
- The possibility of separation of the swell and wind sea data
- Collection of in situ data for example by using a video camera.

Appendix A

Name this Appendix

A.1 Wave characteristics

Ocean surface waves are generated as a result of forces acting on the Ocean. Figure A.1 illustrates the characteristics of waves used to describe the idealized ocean wave:

- Wave height, H, is the vertical change in trough to crest distance.
- Wave amplitude, a, is half wave height.
- Wave length, L, is the crest-to-crest distance (or the distance between two troughs) in meters.
- The Period, T, time of passage of two (successive crests or troughs).
- Steepness, $\frac{H}{L}$, which is the ratio between wave height and wave length.
- Frequency, f, number of crests (or troughs) which pass a fixed point per second. The unit is Hertz (number per second).
- Wave number, K, the number of wavelengths per 2π units of distance given by

$$K = \frac{2\pi}{L}$$

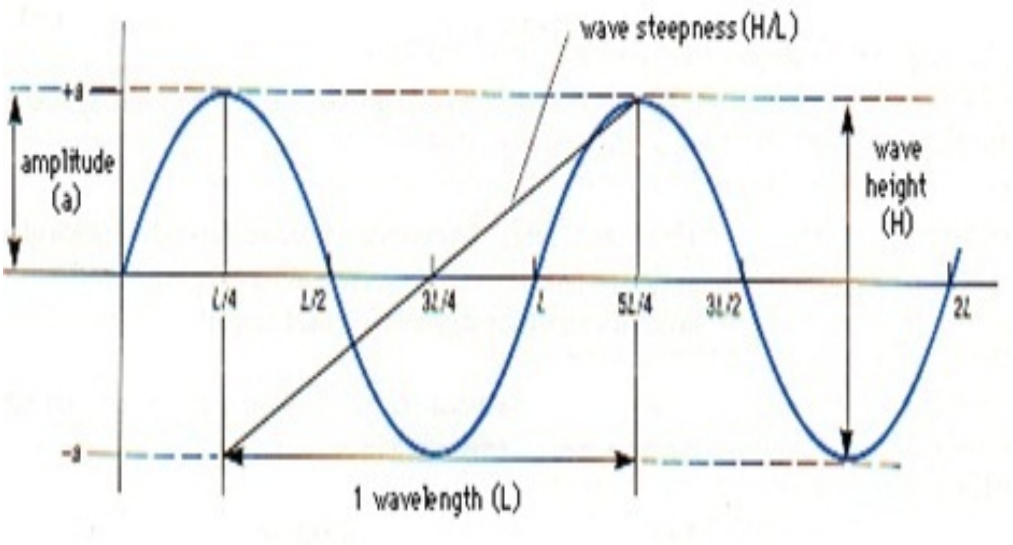

Figure A.1: Basic parameters used to describe a wave.

A.2 Basic relationships

Some assumptions to make a simple wave theory at the surface:

- Using sinusoidal shapes of the wave.
- Small amplitude compare with wave length and depth.
- Viscosity and surface tension can be neglected.
- Large scale forces (e.g. Coriolis force and vorticity) which result from the earth's rotation can be neglected
- Flat bottom (uniform depth).
- None constrained waves or deflected by land masses, or by any other obstruction (Bearman et al., 1989).
- For one dimentional wave :

$$\lambda = cT. \tag{A.1}$$

This equation explains that the wave length is equal to the wave speed times wave period. The first of two Successive waves arrive to reference point after T second,

the second crest will arrive at the same point in the meantime (Laing et al., 1998). Then the propagation of the wave can be described as:

$$\eta(x,t) = a\sin(kx - \omega t). \tag{A.2}$$

In equation (A.2) $k = \frac{2\pi}{\lambda}$ is the wave number and $\omega = \frac{2\pi}{T}$ is the angular frequency. Where x is the independent space variable and t is the independent time variable. The term $(kx - \omega t)$ is called the *wave phase*, c which goes from 0 to 2π for one crest to the next. The speed, c, is the speed at which a point of fixed phase travels, so it is called the *phase speed*.

By using the equation (A.1) and $k = \frac{2\pi}{\lambda}$, $\omega = \frac{2\pi}{T}$, thus, c is:

$$c^2 = \left(\frac{\lambda}{h}\right)^2 = \left(\frac{\omega}{k}\right)^2 = \frac{g}{k}, \tag{A.3}$$

$$\omega^2 = gk. \tag{A.4}$$

The variation of wave speed with wave length is called dispersion, which its variation with angular frequency and the phase speed with the wave number is called dispersion relation. c, is given by the dispersion relation:

$$c^2 = \frac{g}{k}\tanh(kh), \tag{A.5}$$

and

$$\omega^2 = gk\tanh(kh). \tag{A.6}$$

If kh is large (deep water, $h > \frac{\lambda}{4}$), $\tanh(kh) \approx 1$, then

$$c^2 = \frac{g}{k} = g\frac{2\pi}{\lambda}, \tag{A.7}$$

Here, wave speed is controlled by the wave number (k).

Since kh is small in shallow water, $\tanh(kh) \approx kh$

$$c^2 = gh. \tag{A.8}$$

Here, wave speed is controlled by the depth. The wave speed decreases with depth.

Using equation (A.1),

$$T = \sqrt{\frac{2\pi\lambda}{g}}, \text{ and} \tag{A.9}$$

$$\lambda = \frac{gT^2}{2\pi}. \tag{A.10}$$

Appendix B

Matlab code

```
HD=load('indian_Ocean_hs.asc'); % file data of the wave
   height at grid point
y=HD(:,1); % coulomb of year
m=HD(:,2); % coulomb of month
d=HD(:,3); % coulomb of day
h=HD(:,4); % coulomb of hour
time=datenum(HD(:,1),HD(:,2),HD(:,3),HD(:,4),0,0); %
   time series
H0=HD(:,11); %H0 = wave height in deep water
T=load('indian_Ocean_tp.asc'); % file data of time
   period at grid point
Tg=T(:,11);
Lo = (9.81*Tg.*Tg)/(2*pi);
% Lo = wave length at deep water assumed is a same as at
    the beach
% Tg = time period at grid point
R2diss = 0.043*sqrt(H0.*Lo);
% equation of runup dissipative at the beach, assumed
   the slope of the beach is a
% smaller than Irrebarin number (see chapter theory)
```

```
%R2diss = runup dissipation
%L0 = wave length in deep water
%Bf= beach slope
s = 0.35*Bf.*sqrt(H0.*L0);
w = H0.*L0.*sqrt(0.563*Bf.*Bf + 0.004);
R2 = 1.1*(s + w/2);
%R2=non-dissipative runup
X=0:0.10:1.0;
N= histc(R2diss,X);
figure; B=bar(X,N,'histc');
PB=N/sum(N)*100 % histogram of wave runup, where PB is
   the probability
v=load('indian_Ocean_v.asc'); % file data of North-
   suothern wind speed
u=load('indian_Ocean_u.asc'); % file data of East-
   western wind speed
U10 = sqrt(u.*u+v.*v); % U10 = wind component
%u = Eastern wind speed %v= Northern wind speed
for i=1:30680
    fdwh(i)=0.0246*U10(i)^2;
    % fdwh is fully developed wind sea
end
x_mean = [mean_jan,mean_feb,mean_mar,mean_apr,mean_may,
   mean_jun,mean_jul,mean_aug,mean_sep,mean_oct,mean_nov
   ,mean_Dec]; % the Mean of all year
months=['Jan';'Feb';'Mar';'Apr';'May';'Jun';'Jul';'Aug';
   'Sep';'Oct';'Nov';'Dec'];
for i=1:30680
L0(i)=9.8*T0(i)^2/(2*pi);
end
R2D=zeros(30680,1); % initialize vector of runup values
for i=1:30680
```

```
42 R2D(i)=0.043*sqrt(H0(i)*L0(i));
43 end
44 H=0:0.1:3; L=0:10:550; % H-L grid
45 for ih=1:length(H)
46 for il=1:length(L)
47 R(ih,il)=0.043*sqrt(H(ih)*L(il));
48 end
49 end
50 % Runup as a function of wave height and wave length
51 [jl,jh]=meshgrid(L,H);
52 figure; c=contour(jl,jh,R,[0:0.25:2.5]);
53 clabel(c,'manual')
54 hold on; plot(L0,H0,'b.');
55 grid
56 figure; c=contour(jl,jh,R,[0:0.25:2.5]);
57 clabel(c,'manual') hold on; plot(L0,H0,'b.'); grid
```

Bibliography

Al-Salem, K., Rakha, K., Sulisz, W., and Al-Nassar, W. (2005). Verification of a WAM Model for the Arabian Gulf. In: *Arabian Coast Conference, Book of Abstracts, Dubai.* (pp. 27–29).

Ardhuin, F., Chapron, B., and Collard, F. (2009). Observation of swell dissipation across oceans. *Geophysical Research Letters*, **36**(L06607):pp. 1–5.

Battjes, J.A. (1974). *Computation of Set-Up, Longshore Currents, Run-up and Overtopping Due to Wind Generated Waves.* Ph.D. thesis, Delft University of Technology.

Bearman, G., Brown, J., and Open University Oceanography Course Team (1989). *Waves, Tides and Shallow-Water Processes*, volume 4. Pergamon Press.

Caires, S. and Sterl, A. (2005). 100-year return value estimates for ocean wind speed and significant wave height from the ERA-40 data. *Journal of Climate*, **18**(7):pp. 1032–1048.

Clemens, S.C. and Prell, W.L. (1990). Late Pleistocene variability of Arabian Sea summer monsoon winds and continental aridity: Eolian records from the lithogenic component of deep-sea sediments. *Paleoceanography*, **5**(2):pp. 109–145.

Collard, F., Ardhuin, F., and Chapron, B. (2009). Monitoring and analysis of ocean swell fields from space: New methods for routine observations. *Journal of Geophysical Research*, **114**(C07023):pp. 1–15.

Dee, D.P., Uppala, S.M., Simmons, A.J., Berrisford, P., Poli, P., Kobayashi, S., Andrae, U., Balmaseda, M.A., Balsamo, G., and Bauer, P. (2011). The ERA–Interim reanalysis: Configuration and performance of the data assimilation system. *Quarterly Journal of the Royal Meteorological Society*, **137**(656):pp. 553–597.

ECMWF (2006). ERA-Interim . (http://www.ecmwf.int/products/data/software/?track=hotlinks.

Gilhousen, D.B. and Hervey, R. (2001). Improved estimates of swell from moored buoys. In: Edge, B.L. and Hemsley, J.M. (eds.), *Ocean Wave Measurement and Analysis*. volume 200, (pp. 387–393).

Gourlay, M.R. (1992). Wave set-up, wave run-up and beach water table: Interaction between surf zone hydraulics and groundwater hydraulics. *Coastal Engineering*, **17**(1–2):pp. 93–144.

Janssen, P.A.E.M. (2008). Progress in ocean wave forecasting. *Journal of Computational Physics*, **227**(7):pp. 3572–3594.

Kantha, L., Rojsiraphisal, T., and Lopez, J. (2008). The North Indian Ocean circulation and its variability as seen in a numerical hindcast of the years 1993–2004. *Progress in Oceanography*, **76**(1):pp. 111–147.

Komen, G.J., Hasselmann, S., and Hasselmann, K. (1984). On the existence of a fully developed wind-sea spectrum. *Journal of physical oceanography*, **14**(8):pp. 1271–1285.

Kudryavtsev, V.N. and Makin, V.K. (2004). Impact of swell on the marine atmospheric boundary layer. *Journal of physical oceanography*, **34**(4):pp. 934–949.

Kulseng, R. (2010). *100–year in the Mozambique Channel*. Master's thesis, University of Bergen, Geophysical Institute.

Laing, A.K., Gemmill, W., Magnusson, A.K., Burroughs, L., Reistad, M., Khandekar, M., Holthuijsen, L., Ewing, J.A., and Carter, D.J.T. (1998). *Guide to*

Wave Analysis and Forecasting: WMO-No. 702. World Meteorological Organization, second edition.

Massel, S.R. and Pelinovsky, E.N. (2001). Run-up of dispersive and breaking waves on beaches. *Oceanologia*, **43**(1):pp. 61–97.

Miles, J.W. (1957). On the generation of surface waves by shear flows. *J. Fluid Mech*, **3**(Pt 2):pp. 185–204.

Moskowitz, L. (1964). Estimates of the power spectrums for fully developed seas for wind speeds of 20 to 40 knots. *Journal of Geophysical Research*, **69**(24):pp. 5161–5179.

Nielsen, P. and Hanslow, D.J. (1991). Wave runup distributions on natural beaches. *Journal of Coastal Research*, **7**(4):pp. 1139–1152.

Phillips, O.M. (1957). On the generation of waves by turbulent wind. *Journal of fluid mechanics*, **2**(05):pp. 417–445.

Riyaz, A. (2009). *The Information Culture of the Maldives: An Exploratory Study of Information Provision and Access in a Small Island Developing State*. Master's thesis, Curtin University of Technology.

Ruggiero, P., Holman, R.A., and Beach, R.A. (2004). Wave run-up on a high-energy dissipative beach. *Journal of Geophysical research*, **109**(C06025):pp. 1–12.

Sabique, L., Annapurnaiah, K., Balakrishnan Nair, T.M., and Srinivas, K. (2012). Contribution of Southern Indian Ocean swells on the wave heights in the Northern Indian Ocean–A modeling study. *Ocean Engineering*, **43**:pp. 113–120.

Schott, F.A. and McCreary, J.P. (2001). The monsoon circulation of the Indian Ocean. *Progress in Oceanography*, **51**(1):pp. 1–123.

Semedo, A., , Sušelj, K., and Rutgersson, A. (2009). Variability of Wind Sea and Swell Waves in the North Atlantic Based on ERA-40 Re-analysis. In: *Proceedings of the 8th European Wave and Tidal Energy Conference, Uppsala, Sweden, 7-10 September*. (pp. 119–129).

Stochdon, H.F., Holman, R.A., Howd, P.A., and Sallenger, A.H. (2006). Empirical parameterization of setup, swash, and runup. *Coastal Engineering*, **53**(7):pp. 573–588.

Uppala, S.M., Kållberg, P.W., Simmons, A.J., Andrae, U., Bechtold, V., Fiorino, M., Gibson, J.K., Haseler, J., Hernandez, A., and Kelly, G.A. (2005). The ERA-40 re-analysis. *Quarterly Journal of the Royal Meteorological Society*, **131**(612):pp. 2961–3012.

Vitousek, S., Genz, A.S., Barbee, M.M., Fletcher, C.H., and Richmond, B.M. (2010). Pu'ukoholāHeiau National Historic Site and Kaloko-Honokōhau Historical Park, Big Island of Hawai'i. *Technical Report NPS/NRPC/GRD/NRTR–2010/387*, National Park Service, U.S. Department of the Interior, Natural Resource Program Center.

Wang, W. and Huang, R.X. (2004). Wind energy input to the surface waves. *Journal of Physical Oceanography*, **34**(5):pp. 1276–1280.

Woodberry, K.E., Luther, M.E., and O'Brien, J.J. (1989). The wind-driven seasonal circulation in the southern tropical Indian Ocean. *Journal of Geophysical Research*, **94**(C12):pp. 17,985–18,002.

Young, I.R. and Babanin, A.V. (2006). Spectral distribution of energy dissipation of wind-generated waves due to dominant wave breaking. *Journal of Physical Oceanography*, **36**(3):pp. 376–394.